PULSED LASER DEPOSITION OF HYDROXYAPATITE THIN FILMS

A Thesis
Presented to
The Academic Faculty

by

Shevon Johnson

In Partial Fulfillment
Of the Requirements for the Degree
Master of Science in Bioengineering

Georgia Institute of Technology
January 2005

PULSED LASER DEPOSITION OF HYDROXYAPATITE THIN FILMS

Approved by:

Dr. R. J. Narayan, Advisor
School of Materials Science & Engineering
Georgia Institute of Technology

Dr. R. L. Snyder
School of Materials Science & Engineering
Georgia Institute of Technology

Dr. W. B. Carter
School of Materials Science & Engineering
Georgia Institute of Technology

Date Approved: January 2005

ACKNOWLEDGEMENTS

I would like to thank Dr. Snyder and Dr. Narayan for their support and guidance. I would also like to thank Dr. Carter for his time and advice in preparing this thesis. Additionally, I would like to thank Drs. Haluska, Cernatescu and Jin for their assistance with X-ray diffraction and mechanical testing, respectively. I am grateful to Jenny R. Morber for her support and guidance. Finally, I would like to thank my family and friends for their support throughout this project.

TABLE OF CONTENTS

LIST OF TABLES

LIST OF FIGURES

SUMMARY

Pulsed laser deposition (PLD) was used to deposit hydroxyapatite (HA) thin films on various substrates, including silicon (100) and titanium (Ti-6Al-4V) alloy. Thin films of amorphous HA were deposited at room temperature and then annealed over a range of temperatures. The microstructure and composition of the films were determined using scanning electron microscopy (SEM), energy dispersive x-ray spectroscopy (EDS), and X-ray diffraction (XRD). The HA films were found to achieve total crystallinity at 350°C. The mechanical properties of the films were studied by means of nanoindentation and scratch adhesion testing. Crystalline and adherent HA thin films prepared using PLD and post deposition annealing have many potential medical and dental applications.

Keywords: pulsed laser deposition, bioactive ceramics, hydroxyapatite

CHAPTER 1

INTRODUCTION

Hydroxyapatite is a bioactive ceramic that mimics the mineral composition of natural bone. Unfortunately, problems with adhesion, poor mechanical integrity, and incomplete bone ingrowth limit the use of current hydroxyapatite surfaces. In this work, we have developed a novel technique to produce crystalline hydroxyapatite thin films involving pulsed laser deposition and postdeposition annealing.

Chapter 2 provides an overview of conventional bioceramic thin films and their applications. Current challenges in hip replacement are discussed and properties of hydroxyapatite thin films are reviewed. Issues regarding hydroxyapatite film adhesion are addressed.

Chapter 3 describes the experimental procedures for material deposition, postdeposition annealing, and film characterization. Hydroxyapatite films were deposited on Ti-6%Al-4%V alloy substrates by the process of pulsed laser deposition. Film surface topology, chemical composition, and crystal structure were determined using scanning electron microscopy (SEM), x-ray dispersive spectroscopy (XDS), and x-ray diffraction (XRD). Mechanical and adhesive properties were examined using nanoindentation and scratch adhesion testing, respectively. The results of this work are presented and discussed in Chapter 4.

We find that the transformation of hydroxyapatite (HA) from amorphous to crystalline occurs at 350°C. The deposited HA films, both annealed and non-annealed show good adhesion to the Ti-6%Al-4%V alloy substrate. It was also found that the adhesion properties were directly related to the temperature of annealing, with decreasing adhesion strength with increasing annealing temperatures. Other mechanical testing on nanohardness and Young's modulus were also determined for the deposited films. It appears that the adhesion properties of PLD-deposited hydroxyapatite thin films are dependent on postdeposition annealing parameters. It is necessary to improve the adhesion of annealed crystalline hydroxyapatite films.

As a conclusion, the relevance of the current work and future directions are discussed in Chapter 5.

CHAPTER 2

BACKGROUND

Man's intrinsic desires to be active and to challenge his limitations propel research into the improvement of orthopedic interventions. The incidence of orthopedic interventions has increased enormously since man entered the industrial era, largely due to accidents caused by the use of machines, such as farm implements, motor vehicles, and printing presses.

In addition, social awareness of the universal right to existence implies the need to rehabilitate those who are subject to congenital malformations, who have in the past led a life of much lower quality. For this reason the interventions aimed at diminishing orthopedic defects have gone in the direction of reconstructing damaged limb parts. Total hip replacement is one of these interventions. It is of the most revolutionary advances in modern orthopedic surgery, both relieving joint pain and improving joint function.

According the American Academy of Orthopaedic Surgeons, approximately 120,000 hip replacement operations are performed each year in the United States [1]. The high frequency of hip joint replacements can be attributed to the fact that loss of function of the hip joint produces such a severely handicapping condition. Problems with hips are related to the demands on the joint brought about by an upright posture for which evolution has not kept pace. Loads on hip joints as high as 1400 lb must be carried without plastic deformation or fracture.

Prosthetic replacement of the hip is considered when the acetabulum or the head of the femur is damaged by degenerative or destructive conditions. These conditions include osteoarthritis, rheumatoid arthritis, ankylosing spondylitis, avascular necrosis, and persistent pain.

The current implant design is based upon the pioneering work conducted by Sir John Charnley [2]. A cobalt-chromium-molybdenum alloy (ASTM F75), cobalt-nickel-chromium-molybdenum alloy (ASTM F562), or a titanium-aluminum-vanadium-alloy (ASTM F136) surface articulates against an ultrahigh molecular weight polyethylene surface in a total joint prosthesis (see Figure 1). These components are fixed in place using polymethylmethacrylate bone cement.

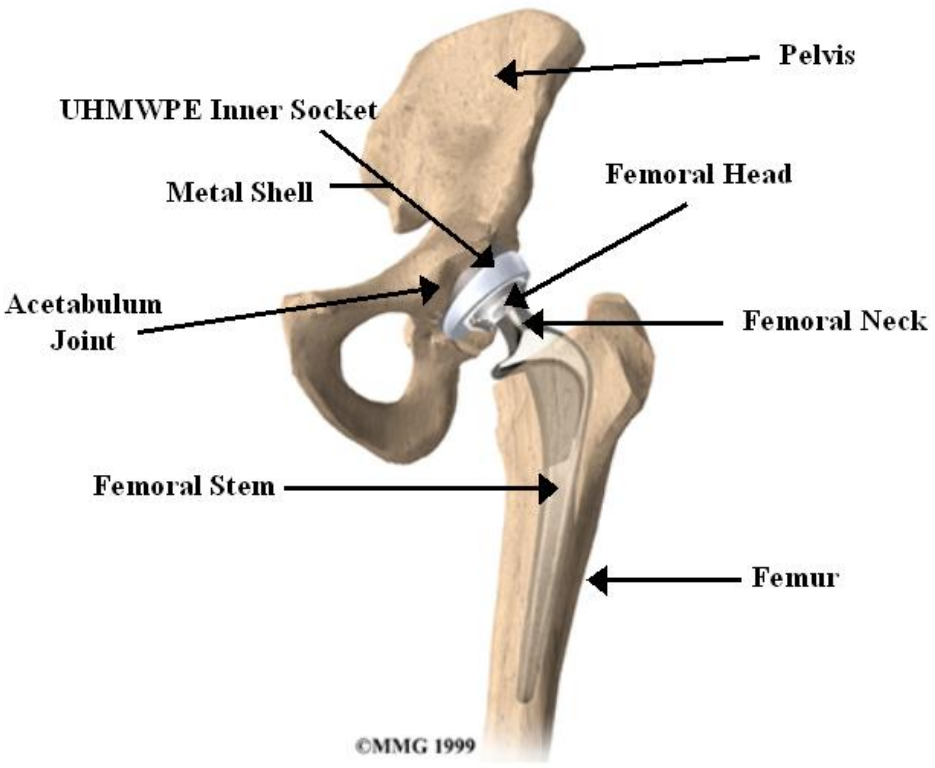

Figure 1: Model of an implanted total hip prosthesis. Modified from MMG [3].

Current devices have exceedingly short lifetimes. It is believed that 10-20% of the implants have to be replaced after 10 years, and some may need to be replaced in as little as 5 years [4]. Loosening, wear, corrosion, uneven stress distributions, and tissue inflammation contribute to these short lifetimes. The relatively poor longevity of these prostheses caused by inadequate cement technology prompted Charnley himself to recommended that total hip arthroplasties be used only in older patients with a limited life expectancy [5].

The polymethylmethacrylate bone cement presents many problems [6]. On one hand, bone cement assists in distributing stresses between bone and metal and can be loaded with antibiotics [7]. Unfortunately, micromotion at the implant-bone interface may lead to the release of a large amount of bone cement particles. Also, stress concentrations at the implant/polymethylmethacrylate interface may lead to polymethylmethacrylate microfracture [8]. Metal, polymer, and bone cement debris can generate third body wear of the metal and polymer prosthesis components. Finally, these wear particles induce inflammation in the surrounding tissues, bone breakdown (osteolysis), and implant loosening.

Wear of orthopedic implant materials is another serious issue. A cobalt-chromium-molybdenum alloy/polyethylene implant generates of a large number of polyethylene wear particles. Polyethylene wear is estimated at 0.10-0.20 mm/year; in fact, some investigators have suggested 100,000 polyethylene particles are released with each step [9]. Wear of the metal component of the joint prosthesis also occurs. For example,

cobalt chromium molybdenum alloy degrades at an average rate of 0.02-0.06 mm in 10 years [10]. Titanium-aluminum-vanadium alloy is more prone to mechanical wear, especially at the titanium-aluminum-vanadium alloy/polyethylene interface [11]. On the other hand, cobalt-chromium-molybdenum alloy particles cause greater tissue toxicity than polyethylene particles or titanium-aluminum-vanadium alloy particles [12, 13].

Stress shielding is another phenomenon that affects joint prostheses. This term refers to an uneven load distribution at the bone-prosthesis interface that can lead to prosthesis loosening [14]. This problem affects every current metal prosthesis component (see Table 1). For example, cobalt-chromium-molybdenum alloy exhibits a modulus of elasticity of 220 GPa [15]. This value is ten times higher than that of the surrounding bone (17 GPa); as a result, stress shielding is quite significant. An alternative metal component material is titanium-aluminum-vanadium alloy. This biocompatible, highly corrosion resistant alloy exhibits a modulus of elasticity of 110 GPa. Unfortunately, titanium-aluminum-vanadium alloy demonstrates poor wear resistance, and exhibits crevice corrosion when fixed using polymethylmethacrylate bone cement.

Table 1: Relevant properties of materials used in orthopedic implants (Modified from Ref [16,17]).

Material	Elastic Modulus (GPa)	Tensile Strength (MPa)	Advantages	Disadvantages
Ti-6Al-4V	124	940	Biocompatibility, corrosion resistance, fatigue strength	Wear resistance
CoCr	214	480	Wear & corrosion resistance, fatigue strength	High modulus, biocompatibility (metal ions)
UHMWPE	0.4	3	Low friction and wear	Soft-susceptible to 3rd body wear, particle creation
PMMA	3	35-50	Rapid fixation, strong fixation for short-term	Low impact and fatigue resistance, biocompatibility
BONE	10-30	70-150	----------	----------

The best replacements for bone have characteristics that approximate those of natural bone. The most desirable mechanism to repair damaged bone is to regrow natural bone by means of tissue engineering. For a relatively large weight bearing joint, tissue engineering of bulk biomaterials is not feasible.

One approach to providing a strong, long-lasting adhesive interface between a bone replacement implant and the surrounding tissue involves the use of bioactive materials [18]. These bioactive materials mimic the behavior of natural bone. Bioactive materials have properties so similar to natural bone that the osteoclasts (bone-dissolving cells) tear down these materials and replace them with natural bone. These materials

include calcium phosphate salts (including hydroxyapatite) and Plaster of Paris (calcium sulfate dihydrate).

Hydroxyapatite (HA) is the most well known bioactive ceramic materials used in medicine [19]. The inorganic constituent of bone is made up of biological apatites, which provide strength to the skeleton and act as a storehouse for calcium, phosphorus, sodium, and magnesium. These biological apatites are structurally similar to the mineral apatites hydroxyapatite (HAp, $Ca_{10}(PO_4)_6(OH)_2$) and brushite (B, $CaHPO_4{\cdot}2H_2O$). At body temperature and in body fluid, two forms of calcium phosphates are stable. At pH < 4.2, the stable calcium phosphate phase is brushite. At pH>4.2, the stable phase is hydroxyapatite.

These apatites, along with fluorapatite (FAp, $Ca_5(PO_4)_3F$), monetite (M, $CaHPO_4$), tricalcium phosphate (TCP, $Ca_3(PO_4)_2$), tetracalcium phosphate (TTCP, $Ca_4(PO_4)_2$), and octacalcium phosphate (OCP, $Ca_8H_2(PO_4)_{6.5}H_2O$) belong to a family of minerals known as apatites. These materials demonstrate similar structures (hexagonal system, space group, P_{63}/m), and possess the structural formula, $X_3Y_2(TO_4)Z$. This structure allows for easy substitution. In nature, apatite compositions include X and Y= Ca, Sr, Ba, Re, Pb, U, or Mn (rarely Na, K, Y, Cu); T = P, As, V, Si, S, or C (as CO_3); and Z=F, Cl, OH, or O. In medicine, apatites of interest possess X=Y=Ca, T=P, and Z=F or OH. For example, the apatite is called hydroxyapatite (HAp) when T=P and Z=OH.

Hydroxyapatite forms crystals that are best described as hexagonal rhombic prisms. The lattice parameters for hydroxyapatite are a=9.432 Å and c=6.881 Å (see Figure 2). Hydroxyl ions (OH-) occur at the corners of the basal plane. These ions are positioned at every 3.44 Å (one half the unit cell), parallel to the c-axis and perpendicular to the basal plane. Thus, 60% of calcium ions in the unit cell are associated with the hydroxyl ions. The density of this material is 3.219 cm^3.

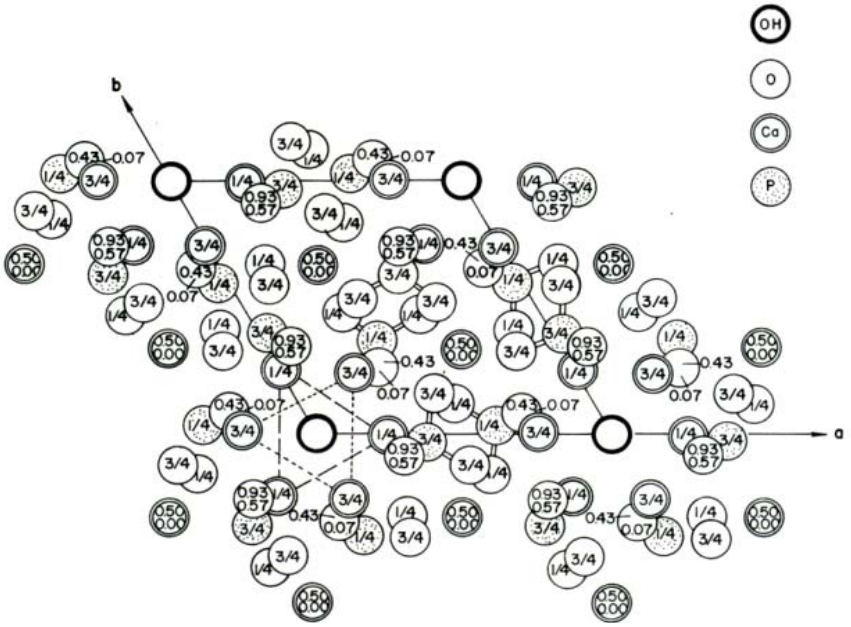

Figure 2. Hydroxyapatite structure projected down c axis onto basal plane [20].

In addition to its similarity to natural bone mineral HA is an osteoconductive material that provides a temporary scaffold for bone growth. The osteoconductive nature of HA coatings results in the formation of strong bonds with bone. The direct contact between living bone and the implant material is known as osseointegration. Brånemark *et al.* originally described the phenomenon in 1977 and later Albrektsson *et al.* defined it in the literature in 1981 [21]. In that paper, Albrektsson *et al.* proposed six factors that are

crucial for successful osseointegration [21]. The osseointegration of a biomaterial depends not only on the properties of the implant material but also on the surface conditions, status of the bone, the surgical technique and the implant loading conditions. Osseointegration has been shown to enhance the reduction of mechanical stresses and micromotions at the bone-implant interface.

Over the years, most clinical practice has been focused on HA coatings deposited by plasma spraying for total hip arthroplasty. In particular, the femoral component has been studied in terms of implant fixation. Implant fixation is assessed by radiographic evidence and by failure rate. Several clinical studies have shown long-term fixation (2-10 years) of the femoral component. The HA coatings were tested based on their initial fixation, stable bone ingrowth and remodeling around the stem. Other studies have revealed that the micromotion of HA-coated stems were comparable to that of cemented stems [22]. Additionally, comparative studies have shown HA-coated stems had a higher survival rate and less bone resorption than the cemented stems [22]. There is a trend in favor of HA-coated stems in terms of improved fixation and durability with respect to uncoated porous implants.

Clinical evaluation of HA coatings on the acetabular component have shown good short-term (2-3 years) results. Radiographic evaluation revealed a reduced rate of migration, low bone resorption, and stable bone ingrowth [22]. However, in long-term studies (3-5 years) HA-coated cups exhibited aseptic loosening [22]. Aseptic loosening has been attributed to long-term mechanical stress assessed by failure rate. In addition,

thick coatings (155±3.5μm) tend to exhibit poor mechanical properties that have been linked to acetabular loosening [22].

The two main failure mechanisms of hydroxyapatite coatings are dissolution and third-body wear. The dissolution of HA coatings depends not only on the pH of the aqueous environment, but also on the composition and crystallinity of the calcium phosphate phases. The rate of dissolution decreases as follows: amorphous HA>>TTCP>α-TCP>OHA>β-TCP>> crystalline HA [18]. In other words, highly crystalline HA is dissolved much slower than amorphous HA. The rapidly dissolving HA coating is resorbed by osteoclasts. The resorption of the coating is integrated into the normal bone remodeling process and is replaced with new bone by osteoblasts cells. The dissolution rate of HA coatings is significant because a rapidly dissolving coating can lead to bone growth [23]. However, this is not always the case. Rapid dissolution rate may lead to fast resorption, loss of fixation, implant loosening and the production of particle debris [23]. Nevertheless, to obtain HA coatings with a predictable calcium phosphate phase, the deposition parameters must be optimized. In addition, the purity and crystallinity of the original HA powder must be controlled to prevent contamination. Highly pure crystalline HA coatings generally result in faster fixation and reduced healing time.

The second mechanism of failure of hydroxyapatite coatings is attributed to third-body wear, which results in osteolysis. Osteolysis is the degradation of the bone caused by osteoclasts, bone resorbing cells. Third-body wear, the generation of polyethylene,

and metallic particles usually occurs at the articulating joint; however, it may also appear around the femoral stem. Mechanical stress placed on the hip implant by the patient is believed to be the source of third-body wear. There is a huge controversy over the effectiveness of HA-coatings in preventing third-body wear. Several clinical studies have revealed no adverse effects of HA coatings and the occurrence of third-body wear. However, other clinical studies have discovered excessive wear at the polyethylene surface due to the accumulation of calcium phosphate and metal particles. The inadequate performance of the HA coating is attributed to the poor mechanical properties resulting from thick coatings (>100μm). The optimal thickness of HA coatings deposited for commercial use is typically between 50-75μm [22].

There are many techniques that have been used to create hydroxyapatite coatings on metallic implant materials. Dip coating, electrophoretic deposition, hot isotatic pressing, pulsed laser deposition, sol-gel processing, and sputter coating have been used to deposit hydroxyapatite coatings (see Table 2).

Table 2. Hydroxyapatite Processing Techniques (adapted from [24]).

Dip Coating	0.05-0.5mm	Can coat complex substrates Requires high sintering temperatures Thermal expansion mismatch is common
Electrophoretic Deposition	0.1-2.0mm	Can coat complex substrates Cannot produce crack-free coatings without difficulty Requires high sintering temperatures
Hot Isostatic Pressing	0.2-2.0mm	HIP cannot coat complex substrates High temperature required, producing thermal expansion mismatch Produces dense coatings
Sol-Gel	<1μm	Complex shapes at low processing temperatures Expensive raw materials
Sputter Coating	0.02-1μm	Line of sight technique Produces amorphous coatings Uniform coating thickness on flat substrates
Thermal Spraying	30-200μm	High processing temperature and rapid cooling leads to amorphous coatings Line of sight technique

Pulsed laser deposition (PLD) is an unique physical vapor deposition (PVD) process that uses a pulsed laser such as KrF to ablate the target material, forming a highly energetic plume that deposits the film onto the substrate. The discovery of the ruby laser prompted an evolution of theoretical investigations into laser-target interaction. Numerous experiments were carried out to verify the theoretical models. Ready (1963) and White (1963) studied the interactions of intense laser beams with solid surfaces [25]. By 1965, Smith and Turner demonstrated that an intense ruby laser could be used to deposit thin films [25]. Since then, PLD has been studied intensively, but it only received major attention when it proved to be a useful technique for the preparation of thin films for high temperature superconductors. The main advantage of PLD is its versatility. Using high-power lasers almost any material can be vaporized and, thus, depositing a thin-film onto any substrate. Cheung and Sankur (1988) are noted to be the first to achieving congruent transfer of material using PLD [25]. In other words, the composition of the any target material can be preserved with in the film. This accomplishment is significant because it proved that PLD could be used to produce thin films with qualities comparable to those produced by Molecular Beam Epitaxy (MBE) [25]. Another very important advantage of PLD is the simplicity of the technique. The laser is completely separated from the actual deposition chamber. During an experiment, the laser beam is pointed onto a target inside the chamber through a viewport in alignment with the target. Under these unique conditions the deposition chamber can contain any working atmosphere.

The pulsed laser deposition technique involves three main steps: ablation of the target material, formation of a highly energetic plume, and the growth of the film on the substrate. A high-power laser is used as an energy source to vaporize a target containing components of the desired film. When the laser radiation is absorbed by a solid surface, electromagnetic energy is converted into electronic excitation as well as chemical, mechanical, and thermal energy to cause evaporation and plasma formation. The ablation of the target forms a plume of energetic atoms, electrons, ions and molecules (see Figure 3). The average kinetic energy of laser-ablated species is typically between 100-1000 kT, where equilibrium energy is on the order of kT [18]. Inside the dense plume, the collisional mean free path is exceptionally small. Immediately after ablation, the plume expands from the target with in vacuum towards the substrate surface.

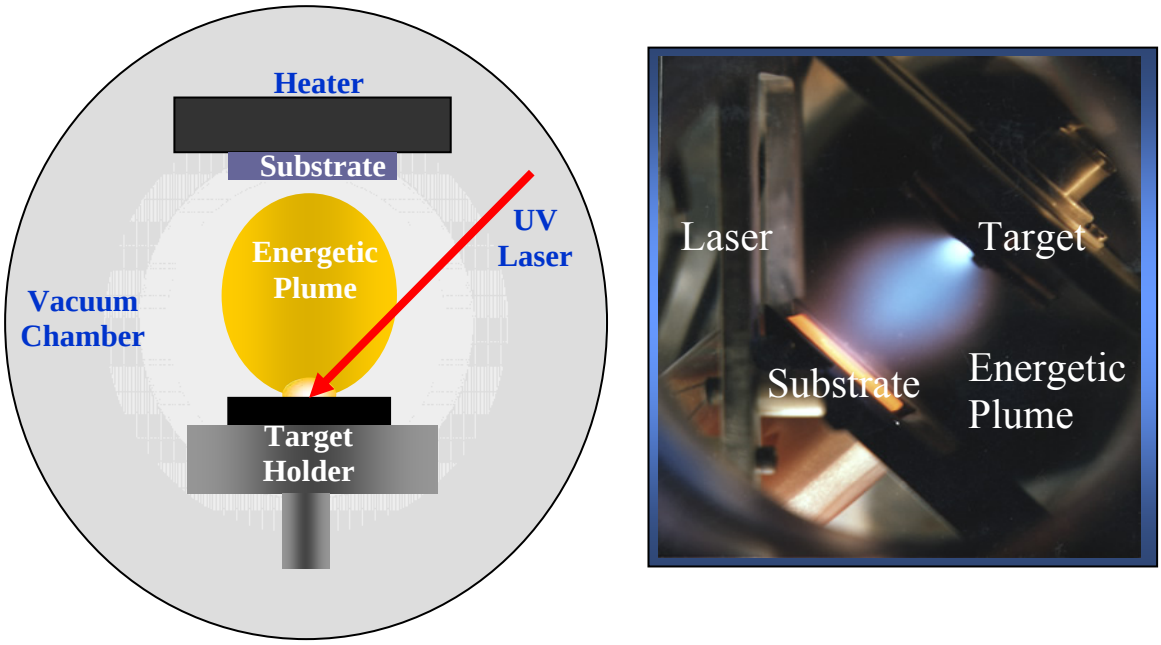

Figure 3: Left Schematic of the PLD process. Right: Photograph of plume during deposition [18].

Thermal spraying is the most common commercial technique for creating hydroxyapatite coatings [26]. However, there are several problems with conventional thermal sprayed coatings. For example, hydroxyapatite is restricted from use in weight-bearing implants, because delamination of the hydroxyapatite film is a common problem. Failure of the hydroxyapatite film can occur at three locations: (1) at the HA/bone interface; (2) between the lamellae in the coatings; or (3) at the HA/metal alloy interface. In vivo studies have correlated the presence of a weak HA/substrate interface with coating delamination. In addition, thermal sprayed hydroxyapatite films contain large numbers of defects, porosity, and cracks; cohesive failure is another possible failure mechanism. The release of hydroxyapatite particles may damage the implant surfaces through third- body wear and inflammation.

PLD has several characteristics that distinguish it from other growth methods and provide special advantages for the growth of chemically complex (multielement) and composite materials [27]. The advantages of technique are the capability for reactive deposition, energetic evaporants, fast deposition times, flexibility, improved film quality at lower temperatures, maintenance of stoichiometry, and simplicity for the growth of multilayered structures.

(1) Congruent (stoichiometric) transfer of material.

The congruent transfer of material is due to the high heating rate and nonthermal albation of the target by a laser-generated plasma. The property of stoichiometric material transfer sets PLD apart from incongruent-transfer methods, such as thermal evaporation

or sputtering. The preservation of stoichiometry depends on two factors, the angular distribution of species and the laser spot size.

(2) Phase purity

The largest advantage of pulsed laser deposition over other hydroxyapatite deposition techniques is the ability to deposit single phase hydroxyapatite films. The deposition temperature and the gas environment can be directly correlated with chemical composition (Ca/P ratio), crystallinity, microstructure, phase, and surface morphology of the deposited film.

(3) Deposition from an energetic plasma beam.

In the plume, exited species have velocities in excess of 10^6 cm/s. The high energies of ablated species can assist film formation, increase film adhesion, and promote chemical reactions between the growing film surface and substrate. The energetic plume particles also enhance film nucleation, surface mobility, and sticking coefficients. These factors when taken together result in improved film quality at lower temperatures.

(4) Capability for reactive deposition in ambient gases.

Energetic species in the plasma react with ambient gases to form oxides, nitrides, and hydrides. Reactive deposition in low pressure gases, including O_2, O_3, NO_2, N_2O, or water vapor, together with the congruent-transfer property, permit the growth of high-quality thin films of multicomponent biocompatible ceramic materials by PLD.

(5) Growth of multilayered epitaxial heterostructures.

In epitaxial thin-film structures, adjacent layers have different compositions, but all layers share a common crystal structure. PLD allows the creation of continuous epitaxial films. A separate target can be used to grow each layer. A multitarget "carousel" is used for easy target exchange. Growth is "digital" because the thickness of each layer can be controlled by calibrating the deposition rate per laser pulse. If one deposits thin films at a low deposition rate (such as 0.1 Å per pulse), it is possible to control film growth at the atomic regime. By increasing the laser pulse rate, commercially attractive growth rates can be achieved.

(6) Deposition rates compare with those observed in molecular beam epitaxy.

The pulsed laser deposition of ceramic materials is a complex process. When the laser beam ablates a target, photons are absorbed by the surface. A molten Knudsen layer is formed, which is a few hundred micrometers thick. The atoms and ions collide within in Knudsen layer. The result of these collisions is expansion perpendicular to the target with velocities ~10^6 cm/s. The vaporization process takes place in a short time with considerable mass transport. A recoil pressure on the liquid layer expels molten droplets of the target. The plasma plume exhibits spherical expansion. The cross section of the plasma stream increases in a geometry similar to that of a de Laval nozzle with negligible exit pressure.

However, there are problems associated with pulsed laser deposition of hydroxyaptite thin films. Previous work suggests pulsed laser deposition of fully

crystalline hydroxyapatite thin films requires temperatures greater than 400˚C and deposition in an Ar/H_2O gas environment. Deposition at lower temperatures produces amorphous films, which resorb too rapidly to provide *in vivo* implant-bone bonding. In addition, films deposited by PLD using an excimer laser on Ti-6%Al-4%V substrates either at room temperature or at elevated temperature in inert gases show very poor adhesion. This may be due to the formation of an intermediate titanium oxide layer between the hydroxyapatite film and the Ti-6%Al-4%V substrate prior to deposition or to softening of the Ti-6%Al-4%V substrate. Mechanisms for lowering the processing temperature must be found to allow pulsed laser deposited-hydroxyapatite films to become clinically relevant implant materials

.

In this study, postdeposition annealing of pulsed laser deposition-grown hydroxyapatite thin films will be examined. High temperature X-ray diffraction was used to determine film microstructure during annealing. The adhesion properties of as-deposited and annealed hydroxyapatite films were compared using microscratch adhesion testing. Surface topology and chemical composition of as-deposited hydroxyapatite films were determined using scanning electron microscopy and energy dispersive spectroscopy, respectively. These novel hydroxyapatite thin films have many potential orthopedic and dental applications.

CHAPTER 3

EXPERIMENTAL PROCEDURES

3.1. Pulsed Laser Deposition

The hydroxyapatite targets were produced from powder supplied by Riedel-de-Haen (Sigma Aldrich, St Louis MO). The powder was hot pressed at 3,000 psi to form 1–inch diameter targets. The targets were sintered at 1,000°C for one hour in a helium atmosphere.

Ti-6%Al-4%V (ASTM F136) stock alloy was cut into 2 mm x 1 cm x 1 cm pieces. Substrates were ground with 240-4000 SiC paper, and polished with 1-μm alumina paste. The polished samples were ultrasonically cleaned in acetone and methanol for five minutes each prior to deposition. Silicon (100) substrates (Silicon Quest International, Santa Clara CA) were cut from a four inch wafer into 2 cm x 2 cm pieces, and ultrasonically cleaned in acetone and methanol for five minutes each prior to deposition. The silicon wafers were etched in a 10% HF solution for five minutes to remove the oxide surface layer. Finally, the Ti-6%Al-4%V alloy and/or Si (100) substrates were mounted onto the substrate heater and loaded into the pulsed laser deposition chamber.

Figure 4 below is a schematic illustration of a typical pulsed laser deposition (PLD) system, the major components of which include a laser source, a high vacuum deposition chamber, and pumping systems. The laser energy density used for deposition

was estimated to be approximately 4-5 J/cm^2. The duration of the laser pulses was 25 ns at a frequency of 10 Hz. The laser spot size was estimated to be 0.043 cm^2. The target-to-substrate distance was maintained at 4.5 cm. All of the depositions were performed at room temperature under vacuum of ~3 x 10^{-6} Pa.

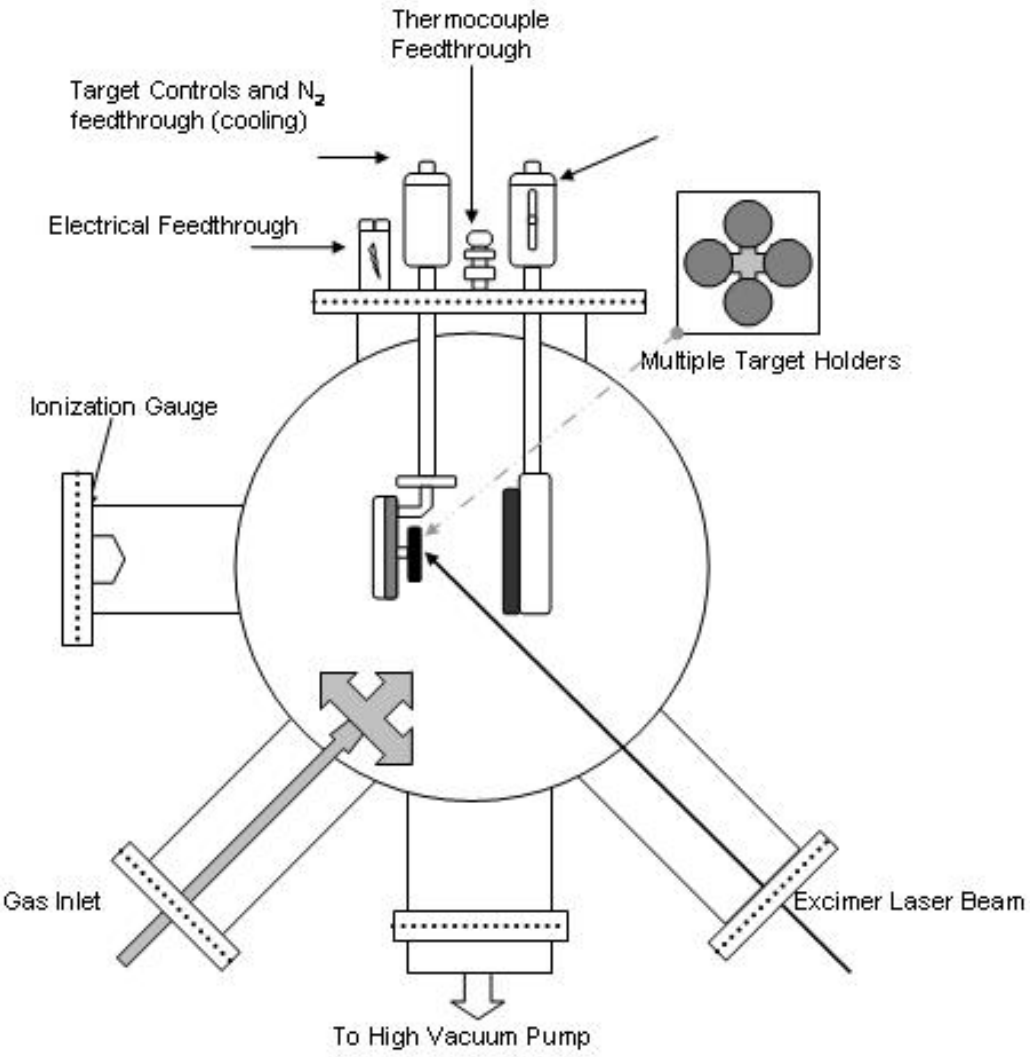

Figure 4. Schematic of Pulsed Laser Deposition system at Georgia Tech [18].

3.2. Scanning Electron Microscopy

Scanning electron microscopy provides a detailed understanding of surface topology, and provides information on film growth. A LEO 1530 Thermally-Assisted FEG Scanning Electron Microscope (SEM) was used to examine as-deposited hydroxyapatite thin films on Ti-6%Al-4%V alloy. This instrument provides 3 nm resolution at 1 kV. The thin window energy dispersive spectrometer (EDS) was used for elemental analysis of the as-deposited hydroxyapatite film. The calcium: phosphate ratio of the as-deposited hydroxyapatite film was compared with the calcium: phosphate ratio in the powder supplied by the manufacturer.

3.3. X-ray Diffraction

High temperature X-ray diffraction (HTXRD) was performed using a Panalytical X-Pert Pro MPD with an Anton-Paar HTK1200 high temperature furnace. Fixed 1/2 degree divergence slits and an Xcelerator detector were used in these experiments. The sample position was calibrated using silicon powder loaded on a silicon substrate, since the as-deposited hydroxyapatite films were amorphous. For HTXRD analysis, hydroxyapatite films were deposited on silicon (100) substrates. In order to eliminate diffraction from the substrate material, a 1˚ω offset was used throughout the measurements. Furnace temperature calibration was done by measuring the thermal expansion of MgO, and comparing the experimental values to the certified values. Diffraction measurements were performed using Cu Kα radiation. Measurements were taken from 10-40˚ 2θ with 10 second count time. Continuous scans were acquired at 50°C temperature intervals. Each diffraction scan took 45 seconds to acquire.

3.4. Nanoindentation

Hardness and modulus measurements of the coatings were performed using an MTS Nanoindenter XP® system (MTS Instruments, Oak Ridge, TN, USA). The direct contact module (DCM) head was used following the standard hardness CSM (Continuous Stiffness Measurement) method. Hydroxyapatite films were deposited on Ti-6%Al-4%V substrates for testing. Mechanical testing was performed on each Ti-6%Al-4%V alloy sample. Indentation depths of 150 nm were employed. Tests were conducted in array of nine indents, each separated by 50 μm. Nanohardness and modulus values were taken from the unloading curves.

3.5. Adhesion Testing

Coating to substrate adhesion was evaluated using the microscratch instrument (CSM Instruments, Irvine CA, USA). A continuously increasing normal load (0-3 N) was applied with a 20 micron diamond tip of Rockwell C geometry. The load of 3 N applied to the circular diamond tip of 20 μm diameter in contact with a flat DLC surface resulted in a maximum Hertzian pressure of 70 GPa. Testing was performed over a scratch length of 2 mm. Critical loads for film cracking and delamination were determined.

CHAPTER 4

RESULTS AND DISCUSSION

4.1. Scanning Electron Microscopy

The surface morphologies of the deposited films were examined using scanning electron microscopy (SEM). The cross-section morphology exhibited a clean, high density coating to substrate interface. The morphology of the coating consists of 1-5 μm droplets and grain-like particles. It is believed that during growth the grain-like particles grow in size and conceal the droplets. The morphology of the droplets suggests that they may be a result of target splashing, since the droplet diameter is much smaller than the particle size of the powder used to prepare the hydroxyapatite target (see Figure 5).

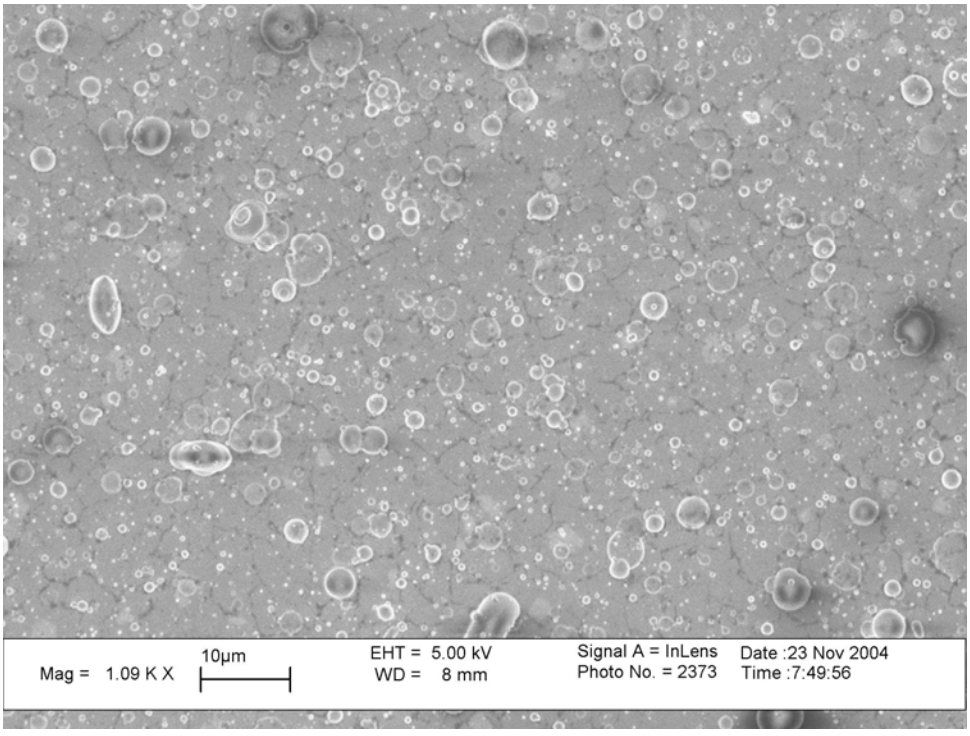

Figure 5. Scanning electron micrograph of a HA film deposited on a Si (100) substrate.

Methods to minimize the particulates include the use of a short-wavelength UV excimer laser and "conditioning" of the target to maintain a smooth surface by a combination of target rotation and laser beam scanning [28]. The most effective active method to reduce particulates is the use of a rotating-vane "velocity filter" that intercepts the large, slow-moving particulates, while transmitting the high-velocity energetic flux to the substrate. This problem can also be solved by optimizing the laser-target interaction; splashing has been minimized by placing the highest possible energy density on the target via optics. In addition, the target may be polished before use to minimize laser interaction with uneven surfaces.

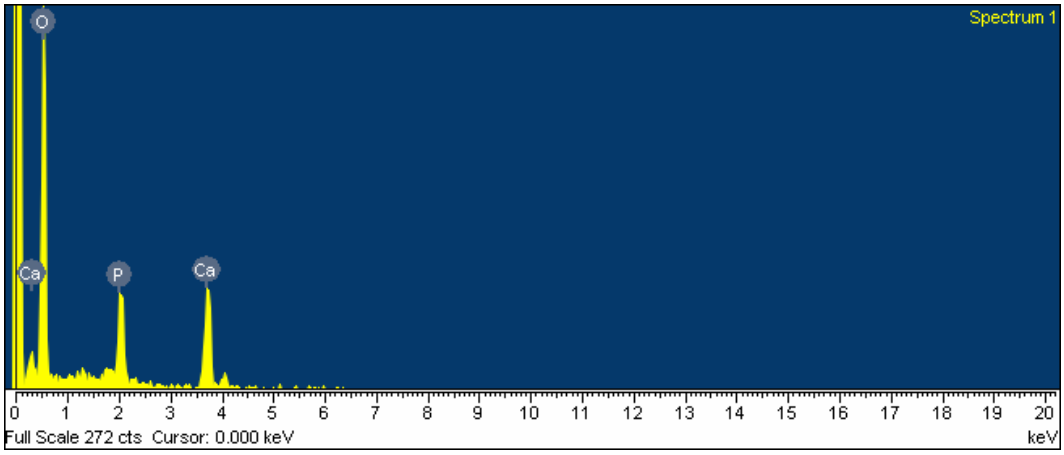

Figure 6. EDS spectrum from a hydroxyapatite film grown on Si (100) substrate.

Figure 6 shows the EDS spectrum from the as-deposited hydroxyapatite film on Si (100). The spectrum shows characteristic peaks corresponding to different elements in the film. The Ca/P weight % ratios for the target and the PLD-deposited film are 2.22 and 3.72, respectively (Table 3). These hydroxyapatite films with higher Ca/P ratios may exhibit greater osteogenic potential [29].

Table 3. EDS Values for PLD-Deposited Hydroxyapatite Film and Target

Material	Ca (Wt. %)	P (Wt. %)	O (Wt. %)
as-deposited HA film on Si (100)	41	11	48
Target	40	18	42

4.2. X-Ray Diffraction

All HA films annealed at temperatures less than 320˚C were amorphous. Typical HTXRD patterns recorded for an incidence angle of 1° are given in Figure 5. Figure 7(a) corresponds to the HA film annealed at 320°C. Figure 7(b) corresponds to the HA film annealed at 330°C. Figure 7(c) corresponds to the HA film annealed at 340°C. Figure 7(d) corresponds to the HA film annealed at 350°C. In Figure 8(a) XRD spectra is shown for the hydroxyapatite target. Figure 9(a) corresponds to the HA film annealed at 300°C. Figure 9(b) corresponds to the HA film annealed at 350°C. Figure 9(c) corresponds to the HA film annealed at 600°C.

It appears that the amorphous to crystalline transformation occurs at 350˚C. Earlier efforts at postdeposition annealing of PLD-deposited hydroxyapatite films involved much higher annealing temperatures. For example, Hontsu et al. describe postdeposition annealing of ArF-deposited HA films at temperatures of 500˚C [30]. Our result suggests that postdeposition annealing and, by extension, pulsed laser deposition of single-phase crystalline hydroxyapatite thin films can be performed at much lower temperatures than previously described. Lower annealing temperatures may mitigate some of causes of poor hydroxyapatite film adhesion.

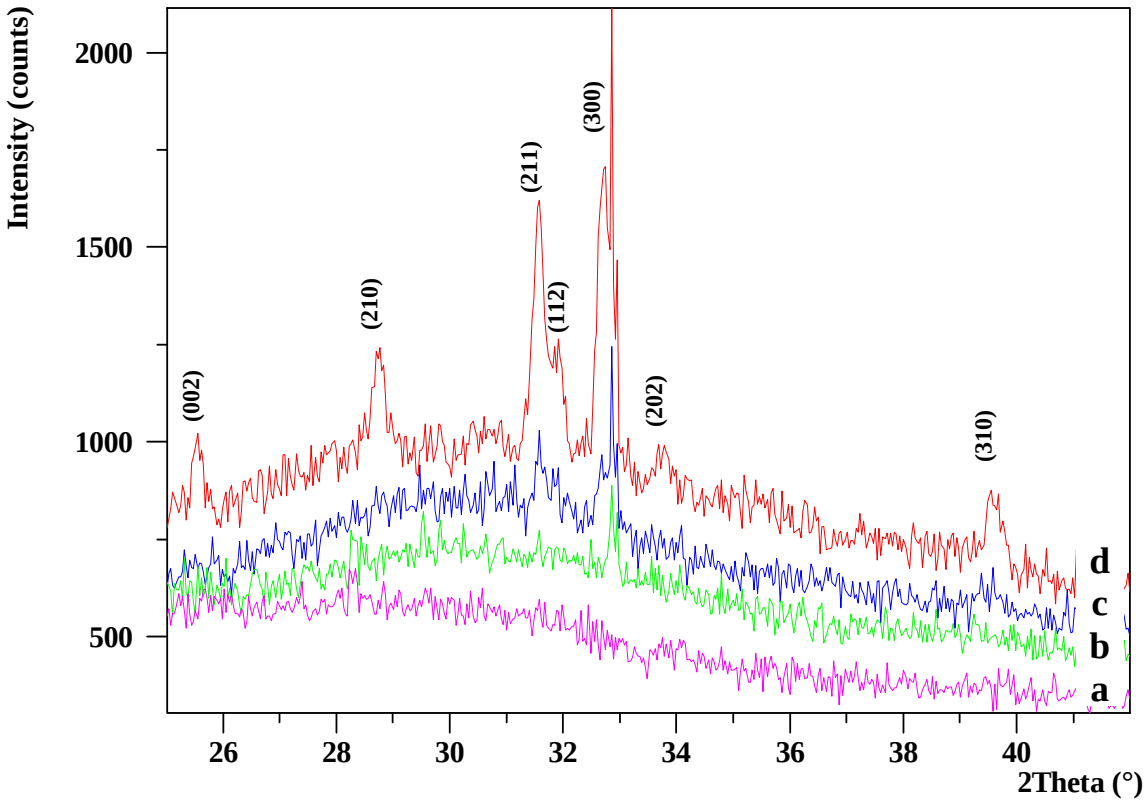

Figure 7. XRD spectra of hydroxyapatite film annealed in the high temperature X-ray diffraction (HTXRD) system. The HTXRD spectra (Cu Kα) was recorded at 1° ω offset for films annealed at (a) 320°C; (b) 330°C; (c) 340°C; (d) 350°C.

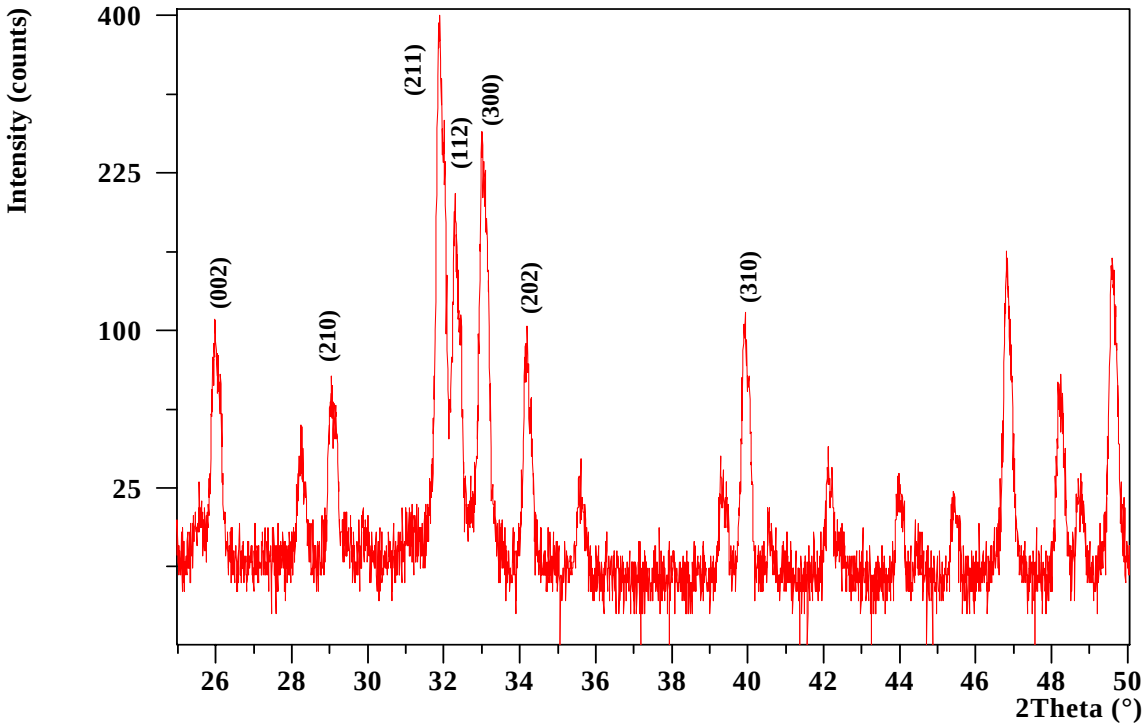

Figure 8. XRD spectra of the hydroxyapatite target.

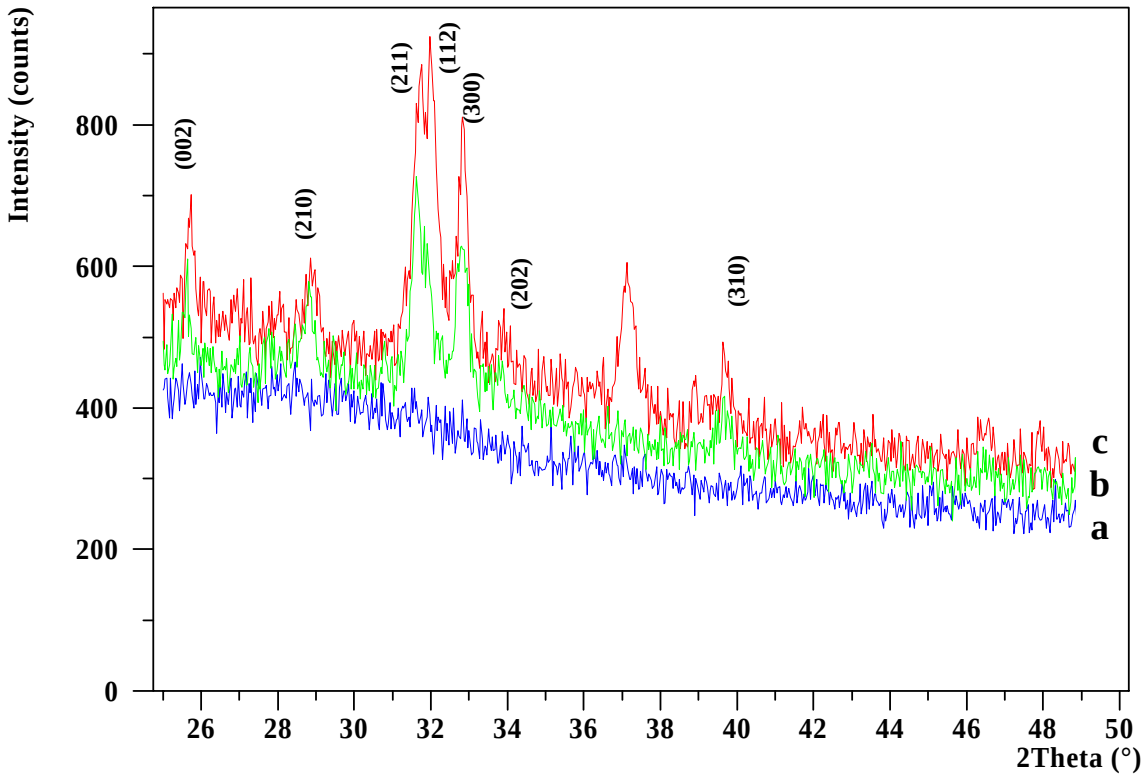

Figure 9. XRD spectra of hydroxyapatite film annealed in the high temperature X-ray diffraction (HTXRD) system. The HTXRD spectra (Cu Kα) was recorded at 1° ω offset for films annealed at (a) 300°C; (b) 350°C; (c) 600°C.

4.3 Nanoindentation

Nanohardness and Young's modulus values for the as-deposited hydroxyapatite film were obtained from the unloading curves. The film exhibits nanohardness and Young's modulus values of 3.48 ± 0.49 GPa and 91.24±20.34 GPa, respectively. These values are similar to those of bulk hydroxyapatite and significantly higher than those of plasma-sprayed hydroxyapatite [31, 32].

4.3. Scratch Test

Scratch adhesion testing is commonly used for determining the integrity of coated substrates. Evaluation of the adhesion between coating and substrate was performed

using a CSM Microscratch instrument. The coating-substrate response to scratch testing may be separated into three regimes. In regime one, mild plastic deformation is observed up to tensile cracking. In regime two, higher loads produce both regular and irregular crack patterns. In particular, regular cracking oblique to the loading direction (cohesive failure) is often observed. Cracks can extend outside the scratch border, in a phenomenon known as external transverse cracking. Cracks may also remain within the scratch track, in a phenomenon referred to as internal transverse cracking. The crack pattern often becomes highly irregular just before the critical load for coating removal is reached. In regime three, coating removal by buckling, delamination, or flaking occurs. First, small amounts of coating debris are observed at the scratch track border. Flaking is enhanced by large friction forces and compressive stresses in the coating ahead of the indenter. Buckling failure may be observed if plastic deformation occurs in the substrate. These scratch adhesion behaviors are highly dependent on the presence of internal compressive stress within the film.

The hydroxyapatite demonstrates very good adhesion, with external transverse cracking observed only at the highest loads in the 600˚C annealed films (see Figure 10). It is interesting to note that the as-deposited and 350˚C annealed films do not exhibit significant external transverse cracking, even at the highest loads (see Figure 10).

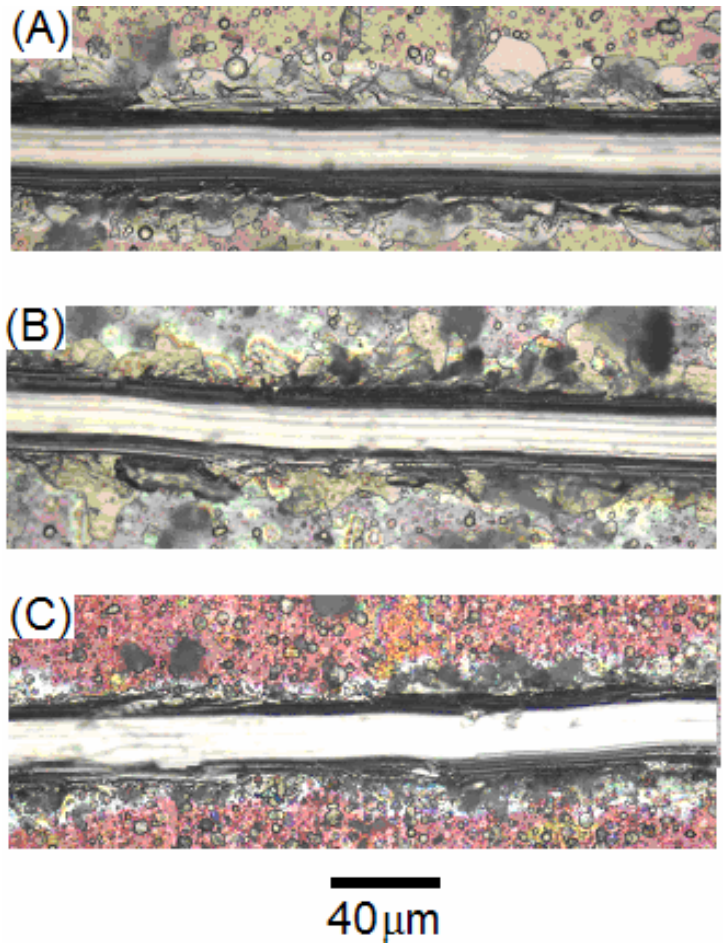

Figure 10. A. As-deposited hydroxyapatite film at 2-3 N load. B. 350˚C annealed film at 2-3 N load. C. 600˚C annealed film film at 2-3 N load.

The total residual stresses in an annealed hydroxyapatite thin film on Ti-6%Al-4%V alloy are composed of intrinsic stresses and thermal stresses. Intrinsic stresses result from microstructure and impurities in the film and occur during the film growth. Lattice-misfit stresses may occur because of a misfit of the lattice parameters. In addition, internal stresses caused by microstructure, such as those caused by trapped point defects (vacancies, interstitials, voids), twins, and dislocations, must be considered.

The coefficients of thermal expansion (CTE) of coating and substrate should ideally match as closely as possible. The coefficient of thermal expansion of hydroxyapatite is somewhat higher than that of the substrate. At room temperature, the thermal coefficient of expansion of hydroxyapatite is approximately 15×10^{-6} K^{-1}. On the other hand, Ti-6%Al-4%V alloy has a thermal coefficient of expansion of approximately 8.8×10^{-6} K^{-1}.

The thermal expansion equations lead to the following conclusions [33]. Consider the situation where (a) the coefficient of thermal expansion of the film ($\alpha(0)$) is different from that of the substrate ($\alpha(s)$), and (b) the films prepared at elevated temperature are cooled ($\Delta T<0$). A tensile stress occurs if $\alpha(0)>\alpha(s)$ Thermal strain $\varepsilon(0)$ in the film, subjected to a temperature differential ΔT, is given by:

$$\varepsilon(0)=\alpha(0)*\Delta T+[F(0)(1-\nu(0))/(\omega*t(0)*E(0))] \quad 10.4$$

and the strain epsilon(S) in the substrate is;

$$\varepsilon(s)=\alpha(s)*\Delta T-[F(0)(1-\nu(s))/(\omega*t(s)*E(s))] \quad 10.5$$

E(0) is the Young's modulus of the film, E(s) is the Young's modulus of substrate, ω is width of the interface, t(0) is the thickness of the film, t(S) is the thickness of the substrate, $\nu(0)$ is the Poisson's ratio of the film, $\nu(S)$ is the Poisson's ratio of the substrate, and F(0) is the interfacial force per unit area.

At the film-substrate interface, the two strains are equal ($\varepsilon(0)=\varepsilon(s)$), and using the above equations, we obtain;

$$F(0)=\omega*(\alpha(s)-\alpha(0))*\Delta T/\{[(1-\nu(0))/t(0)E(0)]+[(1-\nu(s))/t(s)E(s)]\} \quad 10.6$$

$$\text{assuming } t(s)E(s)/(1-\nu(s)) >> t(0)E(0)/(1-nu(0)), \quad 10.7$$

$$\sigma(0)=[F(0)/t(0)]\omega=\sigma(xx)=\sigma(yy)=(\alpha(s)-\alpha(0))*\Delta T*E(0)/(1-\nu(0)) \quad 10.8$$

For hydroxyapatite thin films on Ti-6%Al-4%V alloy substrates, the following situation is observed. On cooling a hydroxyapatite film that has been deposited at 400˚C, the crystalline hydroxyapatite is constrained and is not allowed to shrink. As a result, the cooled film is under tensile stress. Conventional plasma-sprayed hydroxyapatite films suffer from poor adhesion, because these tensile stresses within the hydroxyapatite film have a greater tendency to initiate cracks and cause film delamination. Hydroxyapatite films prepared by room temperature deposition/postdeposition annealing may possess a combination of stresses from lattice misfit, coefficient of thermal expansion, and defect sources. However, it appears that these stresses do not play a significant role in reducing film adhesion.

CHAPTER 5

CONCLUSIONS

The year 2000 brought the inception of the American Academy of Orthopaedic Surgeons “Bone and Joint Decade”. There is a growing recognition of the role of functional bioactive materials in the replacement of diseased tissue. A new technique is proposed for creating crystalline hydroxyapatite thin films using pulsed laser deposition and postdeposition annealing. The amorphous to crystalline transformation occurred at 350˚C. This transition temperature has not been described previously in the literature; previous researchers have prepared crystalline films at significantly higher temperatures. The as-deposited film exhibits nanohardness and Young’s modulus values of 3.48±0.49 GPa and 91.24±20.34 GPa, respectively. Microscratch data revealed that as-deposited films and films annealed at 350˚C demonstrate good adhesion to Ti-6%Al-4%V alloy substrates. These novel coatings have a wide variety of medical applications, including use in orthopedic and dental prostheses.

Future work on hydroxyapatite thin films may take many directions. First, it would be important to replicate these results and transfer this novel processing technique to using other significant medical alloys (e.g., CoCrMo ASTM F75 alloy). In addition, it would be useful to pursue growth functionally graded hydroxyapatite films. These films would contain amorphous hydroxyapatite phases near the film surface and crystalline hydroxyapatite phases near the film/substrate interface. Professor Narayan has worked on functionally graded films using cathodic arc techniques; it would useful to attempt this work using pulsed laser deposition. Laser processing of hydroxyapatite thin films is a very promising research area, in which many challenges remain.

REFERENCES

[1] Neville-Smith M, Trujillo L, Ammundson R. 2000. Special feature: Consistency in postoperative education programs following total hip replacement. Topics in Geriatric Rehabilitation 15: 68-76.

[2] Todd RC, Lightowl CD, Harris J. 1972. Total Hip Replacement In Osteoarthrosis Using Charnley Prosthesis. British Medical Journal 2: 752.

[3] Medical Multimedia Group, M., A Patient's Guide to Artificial Joint Replacement of the Hip. 2002, Montana Spine Center (Appalachian State University): Missoula, Montana.

[4] Birtwistle SJ, Wilson K, Porter ML. 1996. Long-term survival analysis of total hip replacement. Annals of the Royal College of Surgeons of England 78: 180-183.

[5] Emery DFG, Clarke HJ, Grover ML. 1997. Stanmore total hip replacement in younger patients - Review of a group of patients under 50 years of age at operation. Journal of Bone and Joint Surgery-British Volume 79B: 240-246.

[6] Bettencourt A, Calado A, Amaral J, Vale FM, Rico JMT, Monteiro J, Lopes A, Pereira L, Castro M. 2000. In vitro release studies of methylmethacrylate liberation from acrylic cement powder. International Journal of Pharmaceutics 197: 161-168.

[7] Hanssen AD, Spangehl MJ. 2004. Practical applications of antibiotic-loaded bone cement for treatment of infected joint replacements. Clinical Orthopaedics and Related Research 427: 79-85.

[8] Taylor D, Merlo M, Pegley R, Cavatorta MP. 2004. The effect of stress concentrations on the fracture strength of polymethylmethacrylate. Materials Science and Engineering A 382: 288-294.

[9] Schmalzried TP, Campbell P, Schmitt AK, Brown IC, Amstutz HC. 1997. Shapes and dimensional characteristics of polyethylene wear particles generated in vivo by total knee replacements compared to total hip replacements. Journal of Biomedical Materials Research 38: 203-210.

[10] Doorn PF, Campbell PA, Worrall J, Benya PD, McKellop HA, Amstutz HC. 1998. Metal wear particle characterization from metal on metal total hip replacements: Transmission electron microscopy study of periprosthetic tissues and isolated particles. Journal of Biomedical Materials Research 42: 103-111.

[11] Li SJ, Yang R, Li S, Hao YL, Cui YY, Niinomi M, Guo ZX. 2004. Wear characteristics of Ti-Nb-Ta-Zr and Ti-6Al-4V alloys for biomedical applications. Wear 257: 869-876.

[12] MacKinnon N, Crowell KJ, Udit AK, Macdonald PM. 2004. Aluminum binding to phosphatidylcholine lipid bilayer membranes: Al-27 and P-31 NMR spectroscopic studies. Chemistry and Physics of Lipids 132: 23-36.

[13] Rodriguez-Mercado JJ, Roldan-Reyes E, Altamirano-Lozano M. 2003. Genotoxic effects of vanadium(IV) in human peripheral blood cells. Toxicology Letters 144: 359-369.

[14] Karachalios T, Tsatsaronis C, Efraimis G, Papadelis P, Lyritis G, Diakoumopoulos G. 2004. The long-term clinical relevance of calcar atrophy caused by stress shielding in total hip arthroplasty - A 10-year, prospective, randomized study. Journal of Arthroplasty 19: 469-475.

[15] Ratner BD, Hoffman AS, Schoen FJ, Lemons JE. 1996. Biomaterials Science: AN Introduction to Materials in Medicine. 1st edition. Elsevier Science. San Diego, California.

[16] Holand W. 1997. Biocompatible and bioactive glass-ceramics - state of the art and new directions. Journal of Non-Crystalline Solids 219: 192-197.

[17] Long, M. and H. Rack, Titanium alloys in total joint replacement - a materials science perspective. BIOMATERIALS, 1998. 19(18): p. 1621-1639.

[18] Bell, B.F., Functionally graded, multilayer diamondlike carbon-hydroxyapatite nanocomposite coatings for orthopedic implants. 2004. p. x, 92 leaves.

[19] Narayan RJ, Kumta PN, Sfeir C, Lee DH, Olton D, Choi DW. 2004. Nanostructured ceramics in medical devices: Applications and prospects. JOM 56: 38-43.

[20] Posner AS, Perloff A, Diorio AD. 1958. Refinement of hydroxyapatite structure. Acta Crystallica 11: 308-309.

[21] Albrektsson, T. and C. Johansson, Osteoinduction, osteoconduction and osseointegration. European Spine Journal, 2001. 10: p. S96-S101.

[22] Sun, L., et al., Material fundamentals and clinical performance of plasma-sprayed hydroxyapatite coatings: A review. JOURNAL OF BIOMEDICAL MATERIALS RESEARCH, 2001. 58(5): p. 570-592.

[23] Hench, L.L. and J. Wilson, An Introduction to bioceramics. Advanced series in ceramics; v. 1. 1993, Singapore; New Jersey: World Scientific.

[24] Azom. Hydroxyapatite Coatings.http://www.azom.com/details.asp?ArticleID=1405

[25] Cotell, C.M., Thin films and surfaces for bioactivity and biomedical applications: symposium held November 28-29, 1995, Boston, Massachussetts, U.S.A. 1996, Pittsburgh, Pa.: Materials Research Society.

[26] Cheang P, Khor KA. 1996. Addressing processing problems associated with plasma spraying of hydroxyapatite coatings. Biomaterials 17: 537-544.

[27] Sharma AK, Kalyanaraman R, Narayan RJ, Oktyabrsky S, Narayan J. 2001. Carbon nanotube composites synthesized by ion-assisted pulsed laser deposition. Materials Science and Engineering B 79: 123-127.

[28] Rong FX. 1995. Liquid Target Pulsed-Laser Deposition. Applied Physics Letters 67: 1022-1024.

[29] Klein CP, Driessen AA, de Groot K, van den Hooff A. 1983. Biodegradation behavior of various calcium phosphate materials in bone tissue. Journal of Biomedical Materials Research 17: 769-84.

[30] Hontsu S, Matsumoto T, Ishii J, Nakamori M, Tabata H, Kawai T. 1997. Electrical properties of hydroxyapatite thin films grown by pulsed laser deposition. Thin Solid Films 295: 214-217.

[31] Park JB, Lakes RS. 1992. Biomaterials: An Introduction. 2nd edition. Plenum Press. New York, New York.

[32] Yang YC, Chang E, Lee SY. 2003. Mechanical properties and Young's modulus of plasma sprayed hydroxyapatite coating on Ti substrate in simulated body fluid. Journal of Biomedical Materials Research Part 67A: 886-899.

[33] Narayan, R.J., Adhesion properties of functionally gradient diamond composite films on medical and tool alloys. Journal Of Adhesion Science And Technology, 2004. 18(12): p.1339-1365.